SUPERKEKB INTERACTION REGION MODELING

A. Morita, H. Koiso, Y. Ohnishi, K. Oide, H. Sugimoto,
KEK, 1-1 Oho, Tsukuba, Ibaraki 305-0801, Japan

Abstract

In the SuperKEKB interaction region design, the beamline intersects solenoid-axis with large angle and the superconducting final focusing quadrupole magnets are installed into each beamlines without iron-shield. Because of these features, the emittance and dynamic aperture evaluation have to consider the solenoid fringe field and the leakage multipole field of another beamline magnet, respectively. The lattice modeling and the magnetic field handling of both solenoid and multipole field would be reported in this article.

INTRODUCTION

The SuperKEKB[1, 2] is an asymmetric energy double ring collider. It is the luminosity upgrade plan of the KEKB B-factory and its design luminosity is 40 times higher than the achieved luminosity of the KEKB. In order to achieve 40 times luminosity, we introduced a new collision scheme, which use the larger horizontal crossing angle and the smaller transverse beam size at the interaction point(IP), so called nano-beam scheme[3]. For the nano-beam scheme, the final focusing quadrupole doublet design of the SuperKEKB is different to KEKB design. In the following sections, the interaction region(IR) modeling scheme for the SuperKEKB is reported.

INTERACTION REGION OF SUPERKEKB

The configuration of the SuperKEKB IR magnets shown in Fig.1 is different with the KEKB configuration in Fig.2. In the SuperKEKB IR design, the separated superconducting quadrupoles are used for the horizontal final focusing (QC2*) and the vertical final focusing (QC1*) to avoid difficulty caused by the dipole kick of the shared quadrupole magnet like as the KEKB IR. In order to compensate the leakage field from the superconducting quadrupole magnets without the iron yoke on the opposed beamline, the canceler coils for the sextupole, octupole, decapole and dodecapole field are installed. The quadrupole component of the leakage field is used as a help for focusing. The normal and skew dipole kicks by the leakage field are compensated by the steering dipoles in the final focusing magnets. In order to minimize the vertical emittance generated by the solenoid fringe field, the solenoid axis is arranged on the bisection line of the two beamlines. There is no other effective choice, because the vertical emittance generation is proportional with fourth power of the beamline tilt against the solenoid axis. For canceling the solenoid field integral
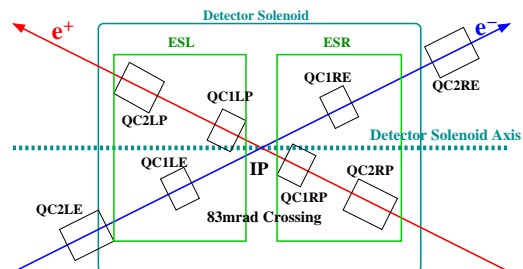

Figure 1: The magnet and orbit layout of the SuperKEKB IR: ESs are the compensation solenoids. QC1s and QC2s are the separated vertical and horizontal focusing superconducting quadrupole magnets, respectively.
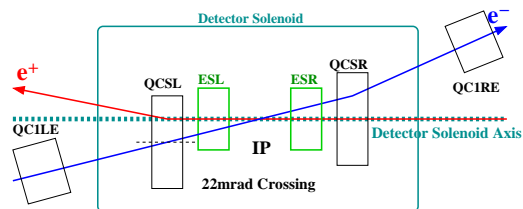

Figure 2: The magnet and orbit layout of the KEKB IR: ESs are the compensation solenoids. QCSs are the shared vertical focusing superconducting quadrupole magnets. QC1s are the additional vertical focusing normal-conducting quadrupole magnets for the electron beam.

from the IP $\int_{IP} B_z(s)ds$, the compensation solenoids are aligned on the detector solenoid axis and are overlaid with the final focusing quadrupoles. The field distribution of the compensation solenoid are optimized for minimizing the solenoid field integral between IP and QC1* and reducing the solenoid fringe effect. For improving the dynamic aperture of the ring, the octupole corrector coils are installed into the final focusing quadrupoles as the non-linear correction knob.

MAGNETIC FIELD MODELING

The magnetic field modeling on the computer is dependent with the beamline element primitives on the computer code. Our accelerator modeling code SAD[4] can handle the multipole element in the solenoid element and can handle the tilt between the multipole axis and the solenoid axis. The field strength is constant in the each slice elements, however, both the multipole and solenoid element have the fringe length parameter and consider the first order deriva-

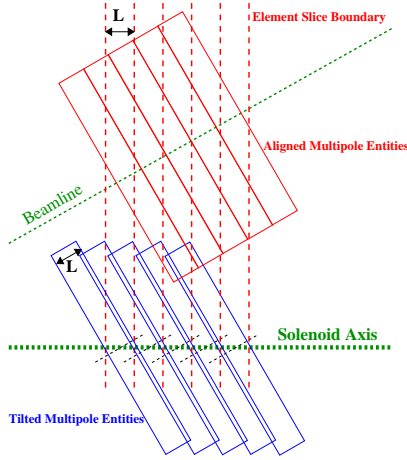01 Circular Colliders

A02 Lepton Colliders

Figure 3: The multipole element boundary and the multipole field location in the lattice modeling: The red dashed-lines show the boundary of the multipole element slice aligned on the solenoid axis. The blue solid boxes show the titled multipole field entities in the element slice. The red solid boxes show the multipole field entities aligned on the beamline.

tive of the magnetic field as the fringe effect. Thus, our modeling correspond to the broken line approximation of the magnetic field distribution and the resolution of the approximation is limited by the thickness of the slices.

For modeling the solenoid region around the IP, we put the solenoid elements based on the common axis of the detector solenoid and the compensation solenoid. The multipole elements of the focusing quadrupoles and the leakage fields which are tilted with the half-crossing angle are aligned on the beamline like as the red solid boxes shown in Fig.3. The horizontal locations of the multipole field entities are adjusted to contact the each boundaries. The coordinate transformation between the element slice boundary and the boundary of the multipole field entity depending with the solenoid field strength makes the discontinuous of the orbit between two adjoining slices which have different solenoid field strength. This is an intrinsic error of the slice modeling with the slice tilting, however, it would not be serious if the solenoid field distribution was smooth.

The algorithm to determinate the modeling parameter are described in the following subsections.

Solenoid Field Modeling

In order to approximate the solenoid field by a series of the solenoid slices, the field strength of the solenoid slice is represented by the average field strength in the solenoid slice and the fringe length at the slice boundary is given by the average of the thickness of the conterminous slices.

Multipole Field Modeling

For approximating the 3-dimensional magnetic multipole field with a series of 2-dimensional multipole slices,

01 Circular Colliders

A02 Lepton Colliders

we fit the 3D magnetic field to the z dependent multipole expansion. The fringe length at the slice boundary is given by the average of the thickness of the conterminous slices same as the solenoid case. On the cylindrical coordinate (r, θ, z), the magnetic scalar potential of the free space $\phi(r, \theta, z)$ is given by

$$\phi(r, \theta, z) = \sum_{n=0}^{\infty} r^n \sin(n\theta + \chi_n)$$
$$\left(\sum_{m=0}^{\infty} \frac{(-1)^m n! r^{2m}}{4^m m! (n+m)!} \frac{d^{2m} d_n(z)}{dz^{2m}} \right) \quad (1)$$

where r and θ are radius and polar angle in the $x - y$ plane $x = r\cos\theta, y = r\sin\theta$. $d_n(z)$ and χ_n are the $2n$-pole field form factor and the rotation angle of the $2n$-pole filed, respectively. The magnetic field $\mathbf{B} = \nabla\phi$ is delivered as follows

$$B_r = \frac{\partial\phi}{\partial r}, \ B_\theta = \frac{1}{r}\frac{\partial\phi}{\partial\theta}, \ \text{and} \ B_z = \frac{\partial\phi}{\partial z}. \quad (2)$$

By using Fourier transformation, θ-direction modes are decomposed as

$$\hat{B}.(n) \equiv \begin{cases} \frac{1}{2\pi}\int_0^{2\pi} B.d\theta & n = 0 \\ \frac{1}{\pi}\int_0^{2\pi} B.e^{-in\theta}d\theta & \text{otherwise} \end{cases}, \quad (3)$$

where $\cdot$ denotes r, θ or z direction. The magnetic field components are described as

$$\frac{\hat{B}_r(n)}{r^{n-1}} = \sum_{m=0}^{\infty} \frac{(-1)^m n!(n+2m)r^{2m}}{4^m m!(n+m)!} \frac{d^{2m}d_n^\dagger(z)}{dz^{2m}} \quad (4)$$

$$\frac{\hat{B}_\theta(n)}{r^{n-1}} = \sum_{m=0}^{\infty} \frac{(-1)^m n! n r^{2m}}{4^m m!(n+m)!}(-i)\frac{d^{2m}d_n^\dagger(z)}{dz^{2m}} \quad (5)$$

$$\frac{\hat{B}_z(n)}{r^{n-1}} = \sum_{m=0}^{\infty} \frac{(-1)^m n! r^{2m+1}}{4^m m!(n+m)!} \frac{d^{2m+1}d_n^\dagger(z)}{dz^{2m+1}}, \quad (6)$$

where $d_n^\dagger(z)$ is the complex form factor $(\sin\chi_n + i\cos\chi_n)d_n(z)$. The real- and imaginary-part of the complex form factor correspond with the skew- and normal-multipole, respectively. By using z-direction Fourier transformation, k_z spectrum of the magnetic fields are obtained as

$$\frac{\tilde{B}_r(n, k_z)}{r^{n-1}} = \tilde{d}_n(k_z) \sum_{m=0}^{\infty} \frac{n!(n+2m)}{(n+m)!} \frac{(k_z r)^{2m}}{4^m m!} \quad (7)$$

$$i\frac{\tilde{B}_\theta(n, k_z)}{r^{n-1}} = \tilde{d}_n(k_z) \sum_{m=0}^{\infty} \frac{n! n}{(n+m)!} \frac{(k_z r)^{2m}}{4^m m!} \quad (8)$$

$$-i\frac{\tilde{B}_z(n, k_z)}{k_z r^n} = \tilde{d}_n(k_z) \sum_{m=0}^{\infty} \frac{n!}{(n+m)!} \frac{(k_z r)^{2m}}{4^m m!}, \quad (9)$$

where $\tilde{d}_n(k_z)$ is the Fourier transformation of the complex form factor $\int_{-\infty}^{\infty} d_n^\dagger(z)e^{-ik_z z}dz$.

The left side of Eq.7-9 is obtained from the magnetic field distribution on the circular cylinder by the Fourier

transformation, and the $\sum_{m=0}^{\infty}$ term in the right side of Eq.7-9 is the function of rk_z that do not depend with the form factor $\tilde{d}_n(k_z)$. Therefore, the spectrum $\tilde{d}_n(k_z)$ is obtained as the de-convolution of the magnetic field spectrum. The obtained complex form factor is the maximum likelihood estimation in the L^2-norm. This scheme could be implemented by the discrete Fourier transformation, if the magnetic field distribution on the $\theta - z$ grid points was given.

For the accelerator code SAD, the integral multipole field strength between $z = z_0$ and $z = z_1$ is defined by

$$K_n \equiv \frac{1}{B\rho} \int_{z_0}^{z_1} \left. \frac{\partial^n B_y}{\partial x^n} \right|_{x=y=0} dz \qquad (10)$$

$$SK_n \equiv \frac{1}{B\rho} \int_{z_0}^{z_1} \left. \frac{\partial^n B_x}{\partial x^n} \right|_{x=y=0} dz , \qquad (11)$$

where K_n, SK_n, and $B\rho$ are the normal $2(n + 1)$-pole field strength, the skew $2(n + 1)$-pole field strength, and the magnetic rigidity, respectively. By using the complex form factor $d_n^\dagger(z)$, Eq.10-11 are rewritten as follows

$$SK_n + iK_n = \frac{(n+1)!}{B\rho} \int_{z_0}^{z_1} d_{n+1}^\dagger(z)dz. \qquad (12)$$

In like manner, the average solenoid field strength of the slice is obtained as

$$BZ \equiv \frac{1}{z_1 - z_0} \int_{z_0}^{z_1} B_z(z)dz \;\; = \left[\frac{d_0^\dagger(z)}{z_1 - z_0} \right]_{z_0}^{z_1}. \qquad (13)$$

In order to obtain longer significant digits, r is desired as larger as possible. The maximum order of the multipole expansion are limited by both the number of samples of θ-grid points and the significant digits of the magnetic field components.

LIFETIME DEGRADATION BY MULTIPOLE FIELD ERROR

The degradation of the Touschek lifetime caused by the multipole field error is estimated by using the dynamic aperture survey based on particle tracking. Figure 4 shows the typical dependency between the multipole error and the increase of the beam loss rate, where the multipole error distributes uniformly around the effective length of the vertical final focusing quadrupole magnet of the positron beam. The multipole field strength shown in Fig.4 is defined as the peak multipole field strength at the physical aperture $r = 10\text{mm}$. In the region that the multipole error is stronger than 0.1mT, the beam lifetime with the most sensitive multipole error is reduced by half.

REMAINING TASKS

Now, the IR magnet design group are introducing the iron yoke into the final focusing magnet design for shielding the leakage field instead of the canceler multipole coils.
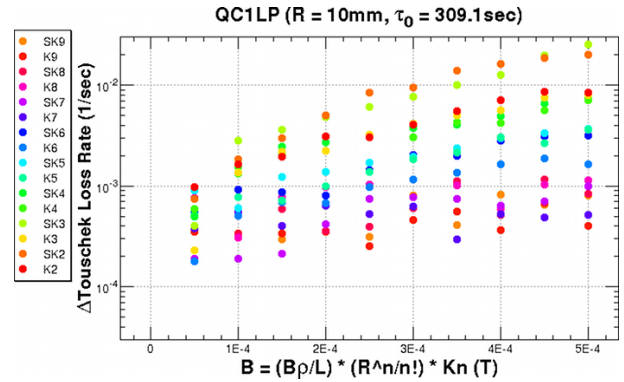

Figure 4: The Touschek beam loss rate caused by the multipole field error on the vertical final focusing quadrupole magnet for the positron beam.

New design reduces the complexity for optimizing many canceler multipole coils, however, the iron yoke breaks the cylindrical symmetry. Therefore the 3D magnetic field calculation for the solenoid is required. And further, the paraxial approximation around the solenoid axis can not be applied to the beamline, because the iron yoke between the solenoid axis and the beamline axis breaks uniformness of the medium.

In order to model the new IR magnet, we prepare the multipole expansion of the 3D solenoid field around the beamline axis for handling the higher order multipole of the tilted solenoid field. It needs two multipole expansions on two different beamlines (one for positron beam and the other for electron beam), however, the multipole expansion for the solenoid can be handled same as the quadrupoles.

SUMMARY

The consistent IR design lattice using the old IR magnet without the iron yoke was constructed. From the multipole error simulation with the old IR model, the threshold of the multipole error for the beam lifetime issue is obtained as about 0.1mT at the physical aperture. In order to follow the IR magnet changes, we are preparing the tool chain for the 3D solenoid field data and waiting the output of the 3D solenoid field calculation. On the other hand, we are using the temporary IR model based on the 2D solenoid field map, which is modified by the hand from the 2D solenoid field calculation result, for the lattice optimization.

REFERENCES

[1] Belle II Technical Design Report, KEK Report 2010-1

[2] M. Masuzawa, "Next Generation B-factories", IPAC 2010, Kyoto, May 2010, FRXBMH01, p. 4764 (2010)

[3] Y. Ohnishi, "Lattice Design of Low Emittance and Low Beta Function at Collision Point for SuperKEKB", IPAC 2011, San Sebastian, September 2011, THPZ007

[4] K. Oide, Nucl. Inst. Meth. A**276**, 427(1989), http://acc-physics.kek.jp/SAD/

01 Circular Colliders

A02 Lepton Colliders